Journal of Medicinal Chemistry

Article

Inhibiting Aberrant Signal Transducer and Activator of Transcription (STAT) Protein Activation with Tetrapodal, Small Molecule Src Homology 2 domain binders: Promising Agents Against Multiple Myeloma

Brent D. G. Page, Danielle C Croucher, Zhihua Li, Yoong Lim Wong, Sina Haftchenary, Victor H Jimenez-Zepeda, Jennifer Atkinson, Paul A. Spagnuolo, Robert Colagouri, andrew martin lewis, Aaron D. Schimmer, Suzanne Trudel, and Patrick Thomas Gunning

J. Med. Chem., **Just Accepted Manuscript** • DOI: 10.1021/jm3017255 • Publication Date (Web): 22 Aug 2013

Inhibiting Aberrant Signal Transducer and Activator of Transcription (STAT) Protein Activation with Tetrapodal, Small Molecule Src Homology 2 domain binders: Promising Agents Against Multiple Myeloma

Brent D. G. Page,[1] Danielle C. Croucher,[2] Zhi Hua Li,[2] Yoong Lim Wong,[1] Sina Haftchenary,[1] Victor H. Jimenez-Zepeda,[2] Jennifer Atkinson,[2] Paul A. Spagnuolo,[2] Robert Colagouri,[1] Andrew M. Lewis,[1] Aaron D. Schimmer,[2] Suzanne Trudel,[2]* Patrick T. Gunning[1]*

[1]Department of Chemical and Physical Sciences, University of Toronto Mississauga, 3359 Mississauga Road, Mississauga ON Canada, L5L 1C6
[2]Ontario Cancer Institute, Princess Margaret Hospital, 620 University Avenue, Toronto, ON, Canada, M5G 2C1

ABSTRACT

The signal transducer and activator of transcription (STAT) proteins represent a family of cytoplasmic transcription factors that regulate a pleiotropic range of biological processes. In particular, Stat3 protein has received particular attention as it regulates the expression of genes involved in a variety of malignant processes including proliferation, survival, migration and drug resistance. Multiple myeloma (MM) is an incurable haematologic malignancy that often exhibits abnormally high levels of Stat3 activity. Although current treatment strategies can improve the clinical management of MM, it remains uniformly incurable with a dismal median survival time post-treatment of 3-4 years. Thus, novel targeted therapeutics are critically needed to improve MM patient outcomes. We herein report the development of a series of small molecule Stat3 inhibitors with potent anti-MM activity *in vitro*. These compounds showed high-affinity binding to Stat3's SH2 domain, inhibited intracellular Stat3 phosphorylation, and induced apoptosis in MM cell lines at low micromolar concentrations.

INTRODUCTION

As a master regulator of cell signaling and tumourigenesis, signal transducer and activator of transcription (Stat) 3 has emerged at the forefront of cancer drug discovery programs.[1-3] Aberrant activation of Stat3 has been observed in a number of solid and haematologic malignancies and is correlated with a variety of hallmark oncogenic processes including cell growth and survival, angiogenesis, inflammation, and metastatic potential.[1-7] Multiple myeloma (MM) is the second most common haematologic malignancy and is responsible for approximately 13 % of blood cancers and 1 % of all cancers.[8] Although MM is generally regarded as incurable, traditional high-dose chemotherapeutics and currently available targeted therapies can improve the prognosis of MM patients when used as part of an aggressive treatment regimen.[8-11] Despite this, the median survival time after conventional treatment remains disappointingly low (3-4 years).[8] In the search for novel molecular targets in MM, Stat3 has emerged as a driving force behind the maintenance and progression of the disease and it is anticipated that Stat3 inhibitors will provide a novel and effective weapon in the fight against MM.[12-14]

The Stat3 signaling cascade is initiated by binding of extracellular ligands such as cytokines and growth factors to their respective cell surface receptors.[1, 4, 15] A subsequent conformational change in the receptor results in intrinsic or kinase-mediated receptor activation via the phosphorylation of key tyrosine residue within the receptor's cytoplasmic domain. These phosphorylated tyrosine residues (pTyr) serve as docking sites for a number of Src-homology 2 (SH2)-domain containing proteins such as Stat3. Thus, the phosphorylated receptor complex recruits unphosphorylated Stat3 via its SH2 domain and in turn Stat3 is activated by

phosphorylation of a C-terminal tyrosine residue (Tyr705). Following dissociation from the receptor complex, phosphorylated Stat3 (pStat3) proteins form transcriptionally active pStat3–pStat3 homo-dimers via reciprocal interactions between the SH2 domain of one activated Stat3 monomer and the pTyr705 of another. Activated pStat3 dimers subsequently translocate to the nucleus, where they bind specific DNA response elements to induce target gene expression. In contrast to the transient nature of Stat3 activation in normal cells, constitutive Stat3 activity, such as that observed in MM, drives the expression of target genes with known oncogenic roles, contributing to the maintenance and progression of tumorigenic processes.

The SH2 domain of Stat3 plays a critical role in the Stat3 signaling cascade, facilitating recruitment of Stat3 to activating cell surface receptors, and playing a key role in the formation of Stat3 homo-dimers.[5, 6, 16] Thus, there has been significant effort to silence aberrant Stat3 signaling by targeting the SH2 domain.[1-4] As a therapeutic target, the SH2 domain of Stat3, like many protein–protein interaction interfaces, is devoid of a classical binding pocket and is relatively flat and hydrophobic.[17, 18] However, the SH2 domain possesses a hydrophilic region (containing residues Lys591, Arg609 and Glu612) responsible for binding to pTyr residues.[18] Many groups, including our own, have targeted this sub-pocket for developing Stat3 inhibitors, employing polar groups such as, phosphate esters,[17, 19-23] catechols,[24] carboxylates[25] and salicylic acids[15, 26-29] that mimic the native pTyr705 substrate. To design Stat3 selective SH2 domain binders, two proximal sub-pockets (one hydrophobic and one amphipathic) have been simultaneously targeted using tripodal Stat3 inhibitors.[25]

Our research group has approached the development of Stat3 inhibitors by performing extensive structure activity relationship (SAR) analysis of a known Stat3-SH2 domain binder, S3I-201 (**1**). This compound was identified through an *in silico* high-throughput screen,[29] and led to the

generation of two lead compounds, **7** and (BP-1-102) **9**, that are now entering advanced pre-clinical trials as cancer therapeutic agents (Table 1).[15, 26, 30]

Table 1: Preliminary SAR leading to the development of lead compounds **7** and **9**.[15, 27] Compound activity was assessed using an electrophoretic mobility shift assay (EMSA) as previously reported.[26, 30]

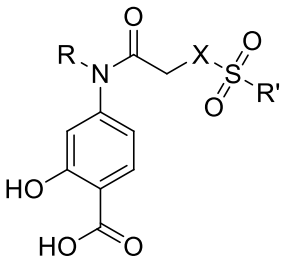

Compound	R	X	R'	IC_{50} (μM)
1	H	O	*p*-Tolyl	84 ± 33
2	H	NH	*p*-Tolyl	> 300
3	H	NCH_3	*p*-Tolyl	> 300
4	H	NBoc	*p*-Tolyl	> 300
5	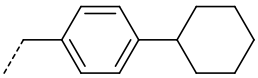	O	*p*-Tolyl	43 ± 13
6	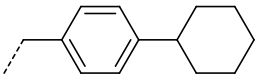	NH	*p*-Tolyl	95 ± 35
7	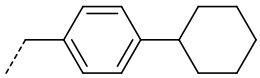	NCH_3	*p*-Tolyl	35 ± 9
8	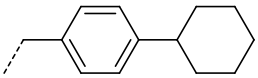	NBoc	*p*-Tolyl	115 ± 35
9	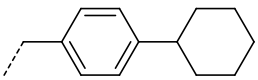	NCH_3	C_6F_5	6.8 ± 0.8

In previous work, we discovered several tripodal inhibitors of Stat3 that have demonstrated promising anti-cancer activity.[26, 30] Using the parent compound **1**, we generated two lead compounds **7** and **9** that have demonstrated more potent Stat3 SH2 domain binding, improved

inhibition of cellular Stat3 activity, and promising activity against cancer cell lines and xenograft models.[15, 27, 30, 31] Interestingly, substitution of the N-methyl group with an oxygen atom, NH or N-Boc resulted in significant changes in inhibitor activity. This prompted further investigation into the sulphonamide nitrogen substituent.

MATERIALS AND METHODS

GOLD Docking Simulations

Inhibitors were docked using GOLD docking software to Stat3 crystal structure, pdb 1BG1. Compounds were first optimized into a low energy geometry. The compound binding site was set to an area with a 12 Å radius surrounding Ser636. Best solutions were visualized using Pymol, which was utilized to create the images shown in Figures 1, 2 and 4C and in supplementary Figure S.1.

Fluorescence Polarization Assay

The fluorescence polarization assay was performed as previously reported. Briefly, fluorescently labelled peptide probe (5-FAM-GpYLPQTV-NH_2, CanPeptide, Pointe-Claire (Montreal), Quebec, Canada) was incubated with Stat3 protein (SignalChem, Richmond, British Columbia, Canada), and inhibitor for 30 minutes then analyzed on a Tecan M1000 fluorimeter (Tecan, Mannedorf, Switzerland). Polarized fluorescence was plotted against concentration of inhibitor and IC_{50} values were determined by fitting to a dose response curve. Representative curves of the top compounds are shown in the supplementary information.

Cell Viability Assays. The MTS and MTT assays were used to measure cellular metabolic activity, which reflects the number of viable cells. Cell**s** were seeded in 96 well plates at 1-3 x

10^4 cells/well in 90 μL of fresh culture medium. Prior to the addition of cell suspensions, 10 μL of test compound (or vehicle control) was added to wells in triplicate. Cultures were then incubated for 72 hours at 37 °C, 5% CO_2. Following treatment, cell viability was assessed by MTS assay (3-(4,5-dimethylthiazol-2-yl)-5-(3-carboxymethoxyphenyl)-2-(4-sulfophenyl)-2H-tetrazolium for AML2, DU145 and MDA468 cell lines, or MTT assay (3-(4,5-Dimethylthiazol-2-yl)-2,5-diphenyltetrazolium bromide for MM cell lines.[15] Relative cell viability (to DMSO control) was determined colorometrically and EC_{50} values determined by fitting to a standard dose response curve when applicable.

Immunoblot Analysis. Following treatment, target cells were harvested and washed twice in ice cold PBS. The resulting cell pellets were lysed in lysis buffer ((50mM Tris-HCl pH 7.4, 150 mM NaCl, 1 mM ethylenediaminetetra acetic acid (EDTA), and 1% NP-40) supplemented with 1 mM phenylmethanesulfonyl fluoride (PMSF), 2 mM sodium vanidate (Na_3VO_4) and protease inhibitor cocktail (Roche Applied Science) for 30 minutes on ice. Protein lysates were collected by centrifugation at 14,000 *g* for 15 minutes. Protein concentration was determined by Bradford Assay (Thermo Scientific, Rockford, IL) and normalized with lysis buffer before the addition of β-mercaptoethanol-supplemented Lamelli sample buffer (Bio-Rad Laboratories, Hercules, CA). Proteins (10-30 μg) were resolved by sodium dodecyl sulfate-polyacrylamide gel electrophoresis (SDS-PAGE) using 7-10% gels, and transferred to polyvinylidene fluoride (PVDF) membranes using wet transfer at 70 V for 1 hour. Membranes were rinsed in Tris-buffered Saline with 0.01% Tween-20 (TBST) and blocked for 1 hour at room temperature in TBST containing 5% bovine serum albumin (BSA) powder, followed by overnight incubation with primary antibodies at 4 °C. Primary antibodies against the indicated proteins were diluted in TBST with either 5% BSA or 5% milk, as specified by manufacturer. Following three 15 minute washes in TBST,

membranes were incubated with horseradish peroxidase-conjugated goat anti-rabbit or anti-mouse secondary antibodies (Thermo Scientific Pierce, Rockford, IL) diluted 1:4000 in TBST for 1 hour at room temperature. Membranes were developed using the enhanced chemiluminescence kit (Perkin Elmer, Waitham, MA) according to the manufacturer's instructions and visualized by autoradiography. Resulting autoradiographs were analyzed by densitometry using the Gel Doc XR station and Quantity One Software (Bio-Rad, Hercules, CA).

Luciferase Reporter Assay

Target cells were transduced with replication incompetent, VSV-g pseudotyped lentiviral particles containing the Stat3-driven *Firefly* luciferase reporter constructs (pCignal Lenti-Stat3$_{TRE}$-FLuc). Transductions were performed with polybrene (8 µg/µl) in accordance with the Cignal Lenti Reporter Assay Kit (SA Biosciences, Frederick, MD). The pCignal Lenti-Stat3$_{TRE}$-FLuc reporter construct is under the control of a basal promoter element (TATA box) joined to tandem repeats of a specific Stat3 transcriptional response element (TRE), and regulates the expression of the mammalian codon-optimized, non-secreted form of the *Firefly* luciferase gene. Stably transduced cells were selected using puromycin (2 µg/µl) for 2 weeks. As an internal control, Stat3*FLuc*-expressing cells were stably transfected with the pCignal Lenti-CMV-RLuc reporter construct, which contains a CMV immediately early enhancer/promoter that constitutively drives *Renilla* luciferase expression. Transductions were performed as previously described and stable cells selected with hygromycin (50 µg/µl) for 2 weeks. *In vitro* reporter construct activity of drug treated cells was measured using the Stop & Glo® Dual Luciferase Assay System (Promega, Madison, WI), with data presented as relative luciferase units (RLU = *Firefly* luciferase/*Renilla* luciferase).

RESULTS

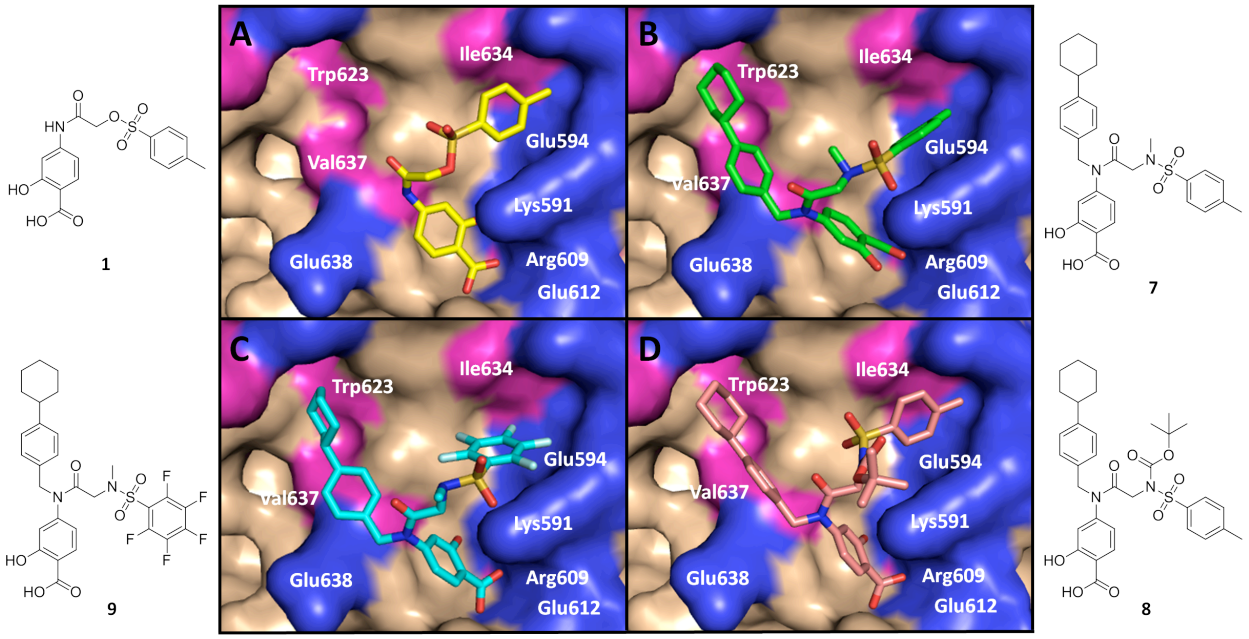

Figure 1. GOLD[32, 33] docking images of compounds bound to Stat3's SH2 domain (Stat3 pdb 1BG1[18]). A: Compound **1**; B: Compound **7**; C: Compound **9**; D: Compound **8**.

Docking simulations were utilized to explore potential binding interactions of compounds **8** which possessed the hydrophobic Boc group appended to the sulfonamide nitrogen. Comparing **8** to parent compounds **1**, **7** and **9**, we observed interesting differences. Compounds **1**, **7** and **9** were found to dock to the SH2 domain of Stat3 with similar conformations as previously reported.[25] We presumed that the salicylic acid group mimics the pTyr motif and facilitated docking with the polar phosphate binding region. The N-cyclohexylbenzyl substituent, common to both **7** and **9**, was found to interact *in silico* with the hydrophobic residues, Val637 and Trp623. The N-methyltoluenesulphonamide group interacted with the amphipathic region which contained Ile634 and Glu594 as well as the hydrophobic side-chain of Lys591.

When the N-Boc derivative (**8**) was docked *in silico*, it was found to orient similarly to **7** and **9**. However, the bulky, hydrophobic *t*-butyl group was found to disfavorably orientate away from the protein surface (Figure 2, A and B). However, this seemingly unfavorable docking position was not reflected in the *in vitro* EMSA disruption assay, with only a slight decrease in potency,[26] and an improved binding affinity observed in the fluorescence polarization (FP) binding assay (Compound **8** IC_{50} = 15.8 ± 0.2 μM *c.f.* compound **7** IC_{50} = 31.0 ± 9.4 μM).

Further docking studies revealed an alternative binding mode for **8** where the Boc group contributed to protein surface binding (Figure 2, C and D). However, unlike previous studies, the N-cyclohexylbenzyl moiety was positioned within the amphipathic binding pocket containing residues Ile634, Glu594 and the side chain of Lys591 (Figure 2). As a result, the substituted sulphonamide group projected into the hydrophobic cleft composed of residues including, Trp623 and Val637. The substituent on the sulphonamide nitrogen interacted with Trp623 and Phe716 and placed the sulfonamide S-substituent in closer proximity to Cys712. This orientation, facilitated by the adoption of the more unfavourable cis amide, allowed for improved interaction between the protein and larger hydrophobic substituent appended to the sulphonamide nitrogen.

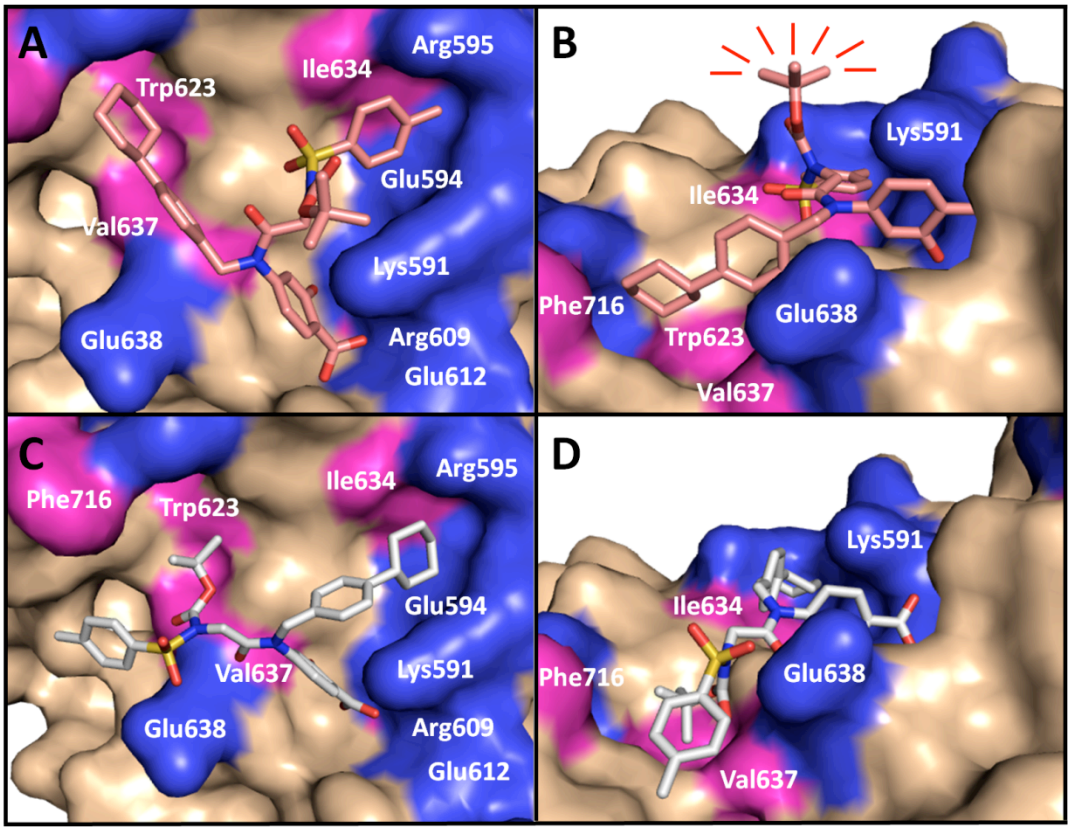

Figure 2. Popular binding modalities of **8** bound to Stat3's SH2 domain (pdb 1BG1[18]). Images A and B show the previously predicted docking poses of **8**. Images C and D show an possible alternative binding mode, where the N-cyclohexylbenzyl and sulfonamide substituents are orientated differently.

To further explore the *in vitro* Stat3 binding potency and whole cell biological effects of N-alkylated analogs of both **7** and **9**, we herein report the synthesis of a novel library of salicylic acid-based inhibitors. Inhibitors were functionalized with select substituents stemming from the sulfonamide nitrogen to furnish a series of tolyl-N-alkyl and perfluorobenzene-N-alkyl derivatives of **7** and **9**, respectively.

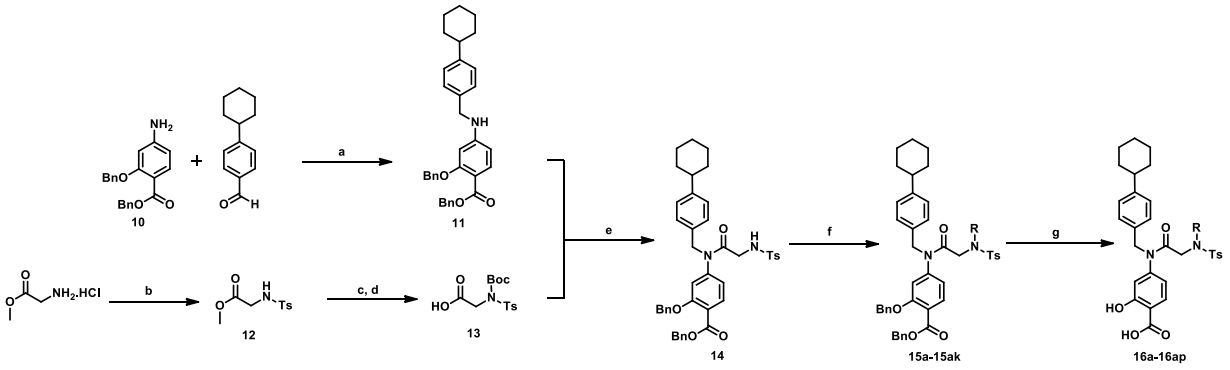

Scheme 1: Synthesis of the tolyl-N-alkyl derivatives. a: i. AcOH, ii. $NaCNBH_3$, MeOH, 6 h, 45 °C; b: TsCl, DIPEA, MeCN, 16 h, 0 °C to RT; c: Boc_2O, DIPEA, CH_2Cl_2, 1 h, RT; d: $LiOH.H_2O$, THF:H_2O (3:1), 16 h, RT; e: PPh_3Cl_2, $CHCl_3$, 0.5 h, 110 °C, microwave; f: RBr or RCl, Cs_2CO_3, DMF, 1 h, RT; g: H_2, Pd/C, THF:MeOH (1:1), 6 h, RT or i. $LiOH.H_2O$, H_2O:THF, 16 h, RT; ii. TFA:toluene (1:1), 1 h, RT.

The tolyl-N-alkyl derivatives were prepared from doubly O-benzyl protected 4-aminosalicylic acid (**10**) which was coupled to 4-cyclohexylbenzaldehyde under standard reductive amination conditions using $NaCNBH_3$. The resultant secondary aniline, **11**, was then coupled to functionalized carboxylic acid, **13**. Carboxylate **13** was prepared from glycine methyl ester hydrochloride which was tosylated using tosyl chloride and then Boc protected using Boc-anhydride. Saponification of the methyl ester gave the acid (**13**) which was coupled to the aniline using triphenylphosphine dichloride. The peptide coupling also cleaved the Boc-protecting group as two equivalents of HCl are generated during this reaction. The sulphonamide nitrogen was functionalized with a variety of alkyl bromides or alkyl chlorides and then deprotected using hydrogenolysis or a step-wise saponification of the benzyl ester followed by treatment with TFA to cleave the benzyl ether. This protocol was used to produce a library of 45 compounds in a divergent fashion. All compounds were subjected to analysis in a

fluorescence polarization (FP) assay and MTS proliferation assay against DU145, MDA-468 and AML2 cells.

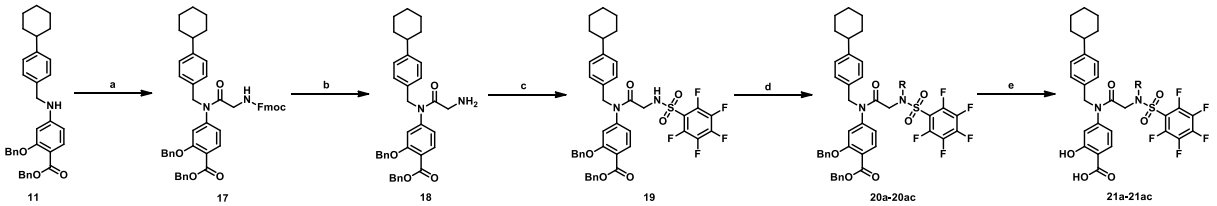

Scheme 2: Synthesis of perfluorobenzene-N-alkyl derivatives. a: PPh_3Cl_2, Fmoc-Gly-OH, $CHCl_3$, 0.5 h, 110 °C, microwave; b: DMF:piperidine (9:1), 0.5 h, RT; c: $C_6F_5SO_2Cl$, K_2CO_3, MeCN, 4 Å MS, 4 h, 0 °C - RT; d: RBr, Cs_2CO_3, DMF, 1 h, RT; e: H_2, Pd/C, THF:MeOH (1:1), 6h, RT.

To make the perfluorobenzene-N-alkyl derivatives, Fmoc-glycine was coupled to secondary aniline, **11**, using triphenylphosphine dichloride. The Fmoc group was removed using piperidine in DMF to afford the free amine. Sulfonamide **19** was prepared by treating amine **18** with pentafluorobenzenesulfonyl chloride. A variety of different alkyl bromides were then used to furnish the sulphonamide nitrogen then treatment with hydrogen and 10% Pd/C gave the deprotected final molecules. Of note, a step-wise deprotection procedure could not be used for the synthesis of the perfluorobenzene-N-alkyl derivatives as treatment with $LiOH.H_2O$ led to nucleophilic aromatic substitution of the perfluorobenzene ring, placing a hydroxyl group *para*-to the sulphonamide substituent. Again, all compounds were subjected to analysis in an FP assay and MTS cell proliferation assay against DU145, MDA-468 and AML2 cells. Selected compounds were further evaluated via Western blot analysis for pStat3 and in MM cell lines for cytotoxicity.

Table 2: Tolyl-N-alkyl Derivatives IC_{50} reported for FP assay.

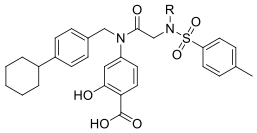

	R	IC_{50} (μM)		R	IC_{50} μM		R	IC_{50} (μM)		R	IC_{50} (μM)		R	IC_{50} (μM)
6		> 50	16g		5.2 ± 0.4	16p		6.0 ± 2.2	16y	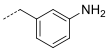	12.4 ± 3.2	16ah		15.4 ± 2.0
7		31.0 ± 9.4	16h		> 50	16q		6.2 ± 0.2	16z	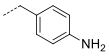	20.8 ± 6.6	16ai		22.8 ± 0.8
8		15.8 ± 0.2	16i		2.8 ± 4.3	16r		7.2 ± 1.0	16aa		45.2 ± 6.0	16aj		8.1 ± 0.6
16a		17.8 ± 2.4	16j	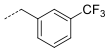	10.2 ± 0.8	16s	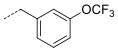	8.0 ± 2.2	16ab		> 50	16ak	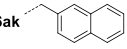	5.0 ± 2.0
16b		17.0 ± 0.6	16k	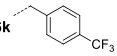	9.2 ± 3.2	16t	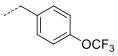	11.8 ± 1.2	16ac		46.6 ± 1.4	16al		11.0 ± 0.8
16c		> 50	16l		10.6 ± 0.6	16u		10.0 ± 3.0	16ad		22.6 ± 1.6	16am	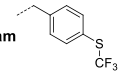	9.6 ± 1.2
16d		> 50	16m	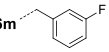	9.0 ± 3.8	16v	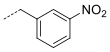	5.0 ± 4.4	16ae	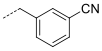	12.4 ± 1.2	16an	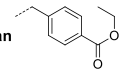	7.6 ± 3.0
16e		14.4 ± 4.4	16n		7.6 ± 3.2	16w	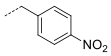	11.0 ± 7.4	16af	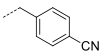	8.6 ± 1.4	16ao	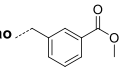	18.4 ± 1.6
16f		8.8 ± 2.9	16o		15.8 ± 0.6	16x		24.0 ± 1.0	16ag		22.2 ± 1.2	16ap	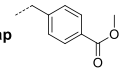	11.6 ± 1.2

Table 3: Perfluorobenzene-N-alkyl derivatives.

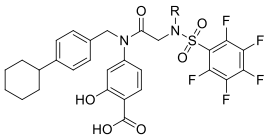

	R	IC_{50} (μM)		R	IC_{50} (μM)		R	IC_{50} (μM)		R	IC_{50} (μM)		R	IC_{50} (μM)
9	CH_3	25.6 ± 0.6	21f		14.6 ± 3.4	21l	F	17.8 ± 0.6	21r	OCF_3	17.8 ± 3.6	21x	F, F, F, F, F	17.6 ± 1.2
21a	H	32.4 ± 4.6	21g		14.4 ± 1.4	21m	F	17.6 ± 1.0	21s	OCF_3	21.6 ± 1.6	21y	F, F, F, F, F	16.6 ± 3.2
21b		20.6 ± 5.2	21h	F_3C	12.8 ± 2.8	21n	Cl	11.0 ± 1.6	21t	NC	11.4 ± 2.2	21z	F, F, F, F, F	11.0 ± 1.6
21c	O, O	27.4 ± 0.8	21i	CF_3	9.6 ± 2.8	21o	Cl	18.2 ± 5.4	21u	CN	19.8 ± 1.4	21aa		21.8 ± 2.6
21d		14.4 ± 1.6	21j	CF_3	22.0 ± 4.8	21p	Cl	13.8 ± 3.4	21v	CN	9.4 ± 3.8	21ab	O, O	17.4 ± 1.0
21e		11.8 ± 2.0	21k	F	28.0 ± 3.2	21q	F_3CO	10.2 ± 2.8	21w	F, F, F, F	12.4 ± 3.6	21ac	O, O, CH_3	30.8 ± 7.0

An FP assay for measuring phosphopeptide:Stat3-SH2 domain disruption was performed as previously reported.[34] Relative to parent compounds (**7** and **9**), many of the N-alkyl derivatives showed improved activity. Moderate improvements were observed through addition of simple alkyl groups. However, it appeared that substituted benzyl substituents provided the greatest enhancement of inhibitory activity. Substitution with the polar pyridine or aminobenzyl appendages led to a marked loss in protein binding affinity. Compounds that incorporated an N-(arylsulfonyl)amide exhibited lower binding affinities, with the exception of the N-Boc analogs.

As a preliminary screen, inhibitors were subjected to an MTS assay to assess the *in vitro* anti-tumour activity of compounds. Most promisingly, a number of these compounds potently inhibited the viability of a range of human cancer cell lines including prostate cancer (DU145), breast cancer (MDA-468) and leukemia (AML2). EC_{50} data and corresponding structures for the

leading five compounds from each family and their corresponding parent structures are summarized in Figure 3. Dose response curves are shown in supplementary information.

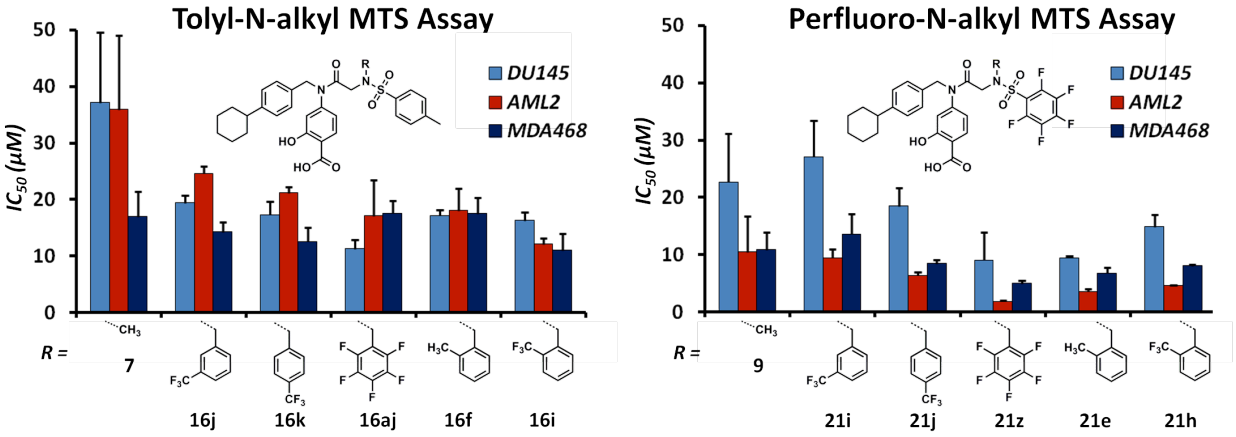

Figure 3. IC_{50} values for the top five tolyl-N-alkyl and perfluoro-N-alkyl compounds as calculated by MTS assay.[15, 26, 27]

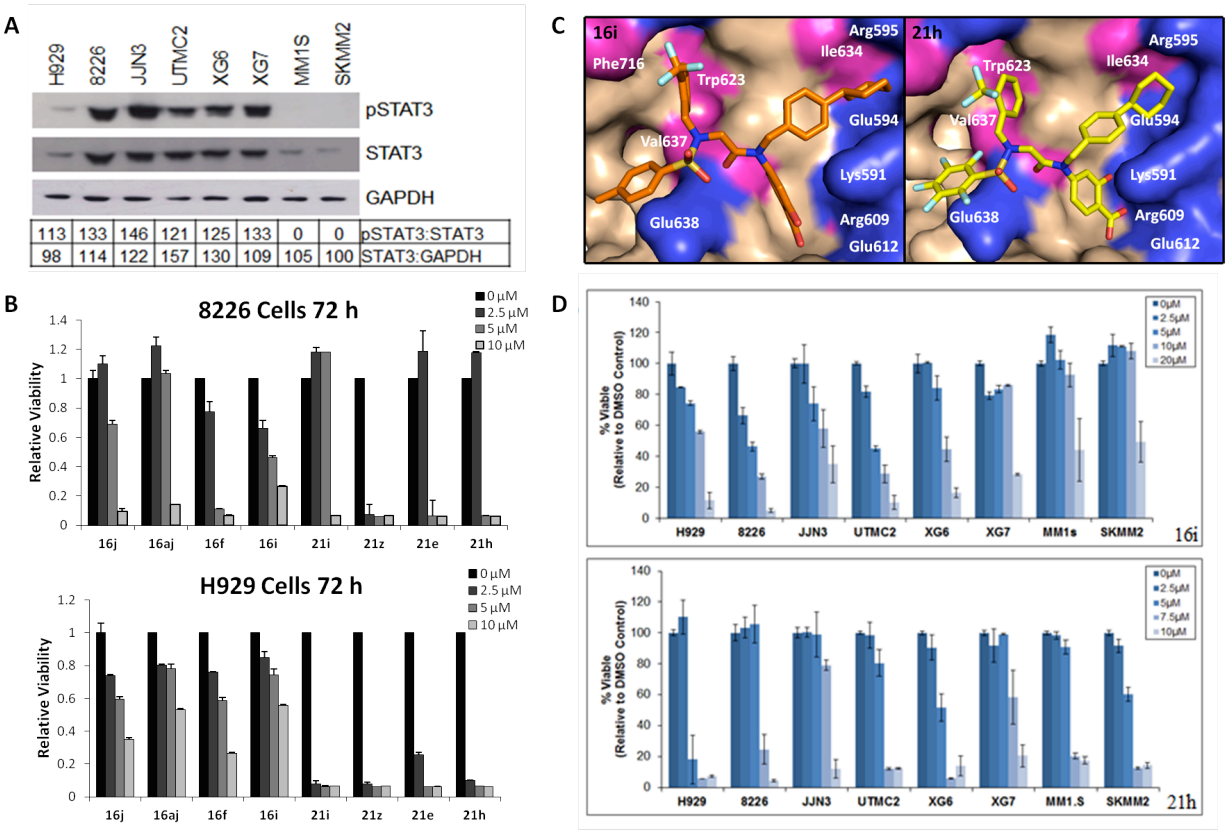

Figure 4. **A**: Western blot analysis of basal pStat3 activation in a panel of human MM cell lines. Quantitative analysis by densitometry shown reveals relative levels of pStat3 to total Stat3 protein, and relative total Stat3 protein to GAPDH. **B**: MTT assay with top eight N-alkylated Stat3 inhibitors against 8226 and H929 MM cell lines. **C**: GOLD docking images of lead compounds **21h** and **16i**. Compounds were found to optimally bind in a similar conformation to compound **8**, suggesting that the N-alkyl group improves binding potency due to a more complete occupation of the Stat3 SH2 domain. **D:** MTT cell viability assay with **16i** (upper) and **21h** (lower) against panel of MM cell lines.

Based on protein binding affinity and inhibition of cell proliferation in DU145, AML2 and MDA-468 cell lines we selected the top eight compounds for further evaluation in the context of MM. We reasoned that lead compounds should demonstrate greater activity against MM cell lines that harbor high levels of pStat3 as they would presumably be more reliant on aberrant Stat3 activity. Therefore, prior to testing lead compound potency, baseline Stat3 activation was first examined in a panel of genetically heterogeneous MM cell lines using Tyr705 phosphorylation as a surrogate marker of Stat3 activation. Whole cell lysates prepared from MM cell lines in logarithmic growth conditions were subject to immunoblot analysis and probed with antibodies against pStat3 (Tyr705) and total Stat3 protein. Although Stat3 protein was expressed in all MM cell lines, albeit to varying degrees, constitutively active pStat3 was detected in 6 of 8 MM cell lines, with two cell lines, MM1.S and SKMM2, lacking detectable pStat3 (Figure 4A). Densitometric analysis performed on immunoblots to quantitate the ratio of pStat3 to total Stat3 protein confirmed variability in baseline pStat3. In the interests of examining the effects of our Stat3 inhibitors, we selected MM cell lines possessing a variety of pStat3 levels for screening lead compounds, predicting that cell lines with high pStat3 should be more sensitive to Stat3 inhibition.

As a preliminary evaluation of anti-MM activity, lead agents were subjected to an MTT assay against two MM cell lines that possessed constitutive Stat3 activation. We selected these two cell lines based on levels of constitutively activated Stat3 protein. A low pStat3 (H929) and a high pStat3 (RPMI-8226) cell line were chosen. We reasoned that cells with lower levels of constitutively active Stat3 would be less sensitive to Stat3 inhibition. Compounds, **16i** and **21h** demonstrated favorable activity and selectivity within their respective libraries and were chosen to undergo further analysis against a larger panel of human MM cell lines.

In docking analyses of inhibitor binding, **16i** and **21h** were found to dock to the Stat3 SH2 domain in a similar orientation to **8**, where the N-alkyl substituents contributed to protein surface binding. Notably, the 2-trifluoromethylbenzyl group interacted with the hydrophobic cleft consisting of residues Trp623 and Val637, while the sulfonamide appendage was projected into a previously unoccupied site containing Cys712, Phe 716 and Glu638. We hypothesized that this interaction may lead to more complete occupation of the Stat3 SH2 domain.

As shown in Figure 4D, both **16i** and **21h** demonstrated dose-dependent inhibition of MM cell viability after 72 hours of treatment, as assessed by MTT assay. Compared with immunoblot analysis of relative baseline pStat3 levels in tested MM cell lines, we noted that **21h**, the pentafluorophenyl-containing analog, showed activity against non-pStat3 containing MM cell lines such as SKMM2 and MM1.s, whereas **16i** exhibited lower biological activity against these cell lines. Moreover, JJN3, which contains high constitutive Stat3 activation, was more resistant to **21h** than **16i**. Notably, these compounds were approximately two-fold more potent than parent compounds **7** and **9** (data not shown). Taken together, these findings suggested that the potent anti-MM activity of **21h** may be, at least in part, due to off-target effects, whereas **16i** delivered a more desirable activity profile and will likely provide a larger therapeutic window. Alternatively, the broad activity of **21h** against this panel of MM cell lines, regardless of baseline Stat3 phosphorylation status, may reflect a universal dependence of MM tumour cells on non-canonical Stat3 signaling pathways that are dependent on a functional SH2 domain, but not Stat3 phosphorylation.

Given the activity profiles of **16i** and **21h** in MM cell lines, we next evaluated the ability of these compounds to inhibit Stat3 phosphorylation. Exposure to **16i** and **21h** for 6 hours lead to dose-dependent inhibition of pStat3, and as expected, no inhibition of total Stat3 protein levels (Figure

5A). As Stat3 is a master transcriptional regulator, we also employed a Stat3-driven luciferase reporter construct to evaluate Stat3 transcriptional activity. In agreement with inhibition of Stat3 phosphorylation, treatment with **16i** and **21h** potently inhibited the transcriptional activity of Stat3 in 8226 and XG6 cell lines, with reductions in relative luciferase ranging from approximately 50-80% after 6 hours (Figure 5B). For **16i**, the observed inhibition of transcriptional activity correlated well with the initial MTT results. Conversely, treatment with 7.5 μM of **21h** had little effect on luciferase production, however, dosing **21h** at this concentration had potent biological effects in the MTT assay. These results suggested that while both **16i** and **21h** inhibited Stat3 phosphorylation and transcriptional activity, the increased cellular activity of **21h** may be due to off-target effects.

To evaluate whether **16i**/**21h-**mediated inhibition of Stat3 phosphorylation and transcriptional activity was sufficient to abrogate downstream Stat3-induced gene expression, we evaluated the effect of these compounds on a known Stat3 target gene, c-Myc. Since this particular protein is known to have a very short half-life (20-30 minutes),[35] we evaluated the resulting effects of drug treatment on c-Myc protein expression after 6 hours using immunoblot analysis. Consistent with the previously observed decreases in Stat3 transcriptional activity, both **16i** and **21h** dose-dependently reduced c-Myc protein expression (Figure 5A). However, in a separate analysis, negligible decreases were observed in other known Stat3 targets such as Bcl-xL and survivin (data not shown), which we speculate to be a result of differences in protein-specific kinetics.

To further confirm the induction of apoptosis following treatment with **16i** and **21h**, whole cell lysates of inhibitor treated JJN3 cells were collected and subjected to immunoblot analysis for cleaved Poly ADP-ribose polymerase (cPARP), a marker of apoptosis. As shown in Figure 5A, both **16i** and **21h** induced PARP cleavage.

To further characterize the cellular activity of **16i** and **21h** and the mechanisms by which they effect MM cell viability, we evaluated **16i** and **21h** induced apoptosis using flow cytometric analysis of Annexin V and PI staining. In 8226 cells, both **16i** and **21h** induced apoptosis in a dose- and time-dependent manner as represented by a shift of cells from the lower left quadrant (viable cells), to the lower right quadrant (early apoptotic cells) at 24 hours, and migration to the upper right quadrant (late apoptosis) at 48 hours (Figure 5C). Promisingly, analysis of apoptosis in MM cell lines with varying degrees of sensitivity to **16i** and **21h** revealed similar results to those observed in the MTT assay, with a greater induction of apoptosis in 8226 cells compared to XG6 and JJN3 cells (Figure 5D).

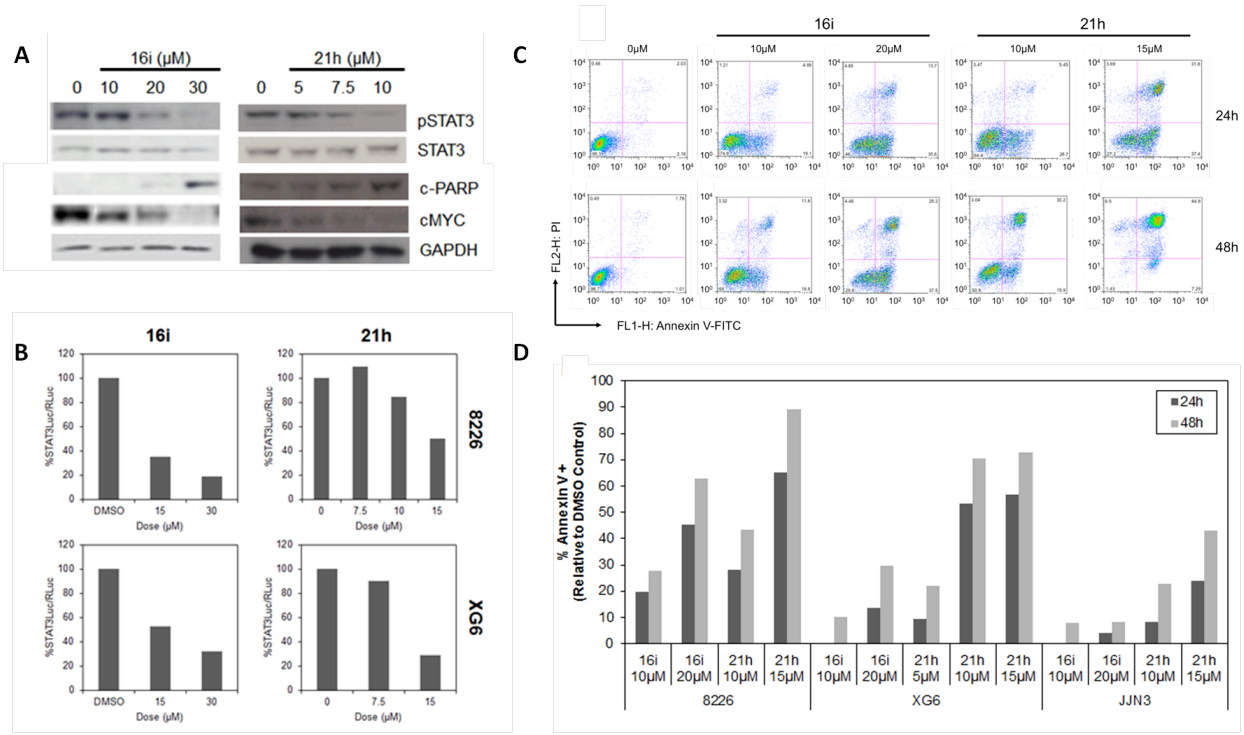

Figure 5. A: Western blot analysis of **16i-** and **21h-** mediated effects on pStat3 inhibition in JJN3 tumour cells, revealing dose-dependent inhibition of Stat3 phosphorylation, inhibition of Stat3 target gene expression as demonstrated by c-Myc and induction of apoptosis shown by

increased PARP cleavage. **B**: Luciferase assay demonstrating that after 6 hours, both **16i** and **21h** dose dependently inhibit Stat3-driven luciferase expression. **C**: Flow cytometric analysis of **16i-** and **21h-** mediated apoptosis as measured by Annexin V and PI staining. Representative scatterplots for 8226 cells showing increased population of cells in the lower right quadrant after 24 hours of treatment, which migrate to the upper right quadrant after 48 hours. **D:** Analysis of apoptosis in 8226, XG6 and JJN3 human MM cell lines upon treatment with **16i** and **21h**.

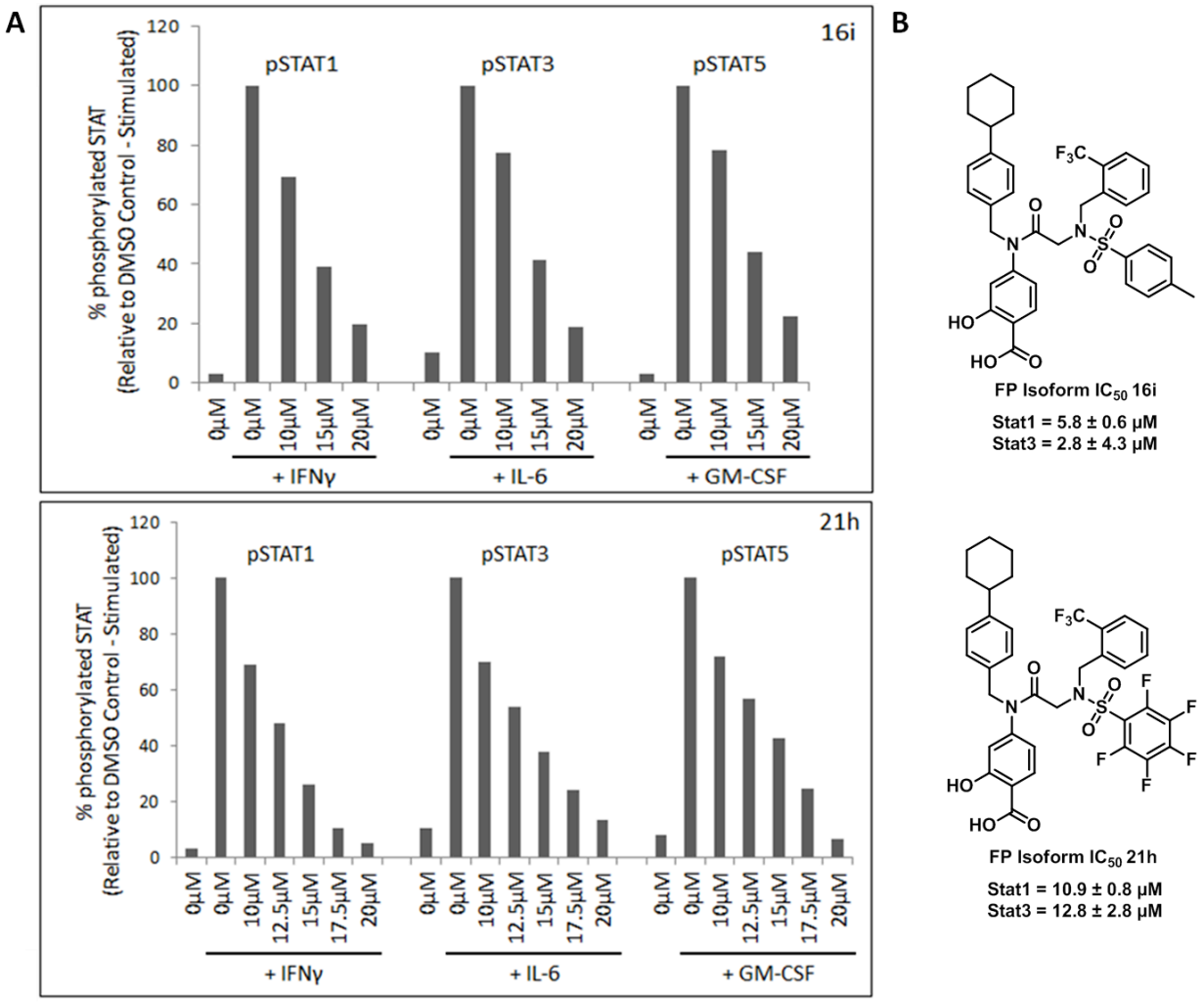

Figure 6. A: Analysis of **16i** and **21h** selectivity for cytokine-induced STAT phosphorylation. Serum-starved U937 cells were treated with **16i** or **21h** for 4 h prior to stimulation with indicated cytokine for 15 minutes. Graphical comparison of **16i** and **21h** selectivity for inhibiting Stat1, 3, and 5 phosphorylation as assessed by phospho-flow cytometry. **B**: Fluorescence polarization assays with Stat1, Stat3 and Stat5 were conducted with lead inhibitors **16i** and **21h** to investigate isoform selectivity.

To address the selectivity of these compounds for inhibiting Stat3 over other STAT isoforms in cells, we performed phospho-flow cytometry to investigate the effects of these compounds on cytokine-induced Stat1/3/5 phosphorylation. Although both **16i** and **21h** were shown to inhibit IL-6-induced Stat3 phosphorylation in these experiments, similar levels of inhibition were also observed for GM-CSF-induced Stat5 phosphorylation and IFNλ-induced Stat1 phosphorylation (Figure 6A). Limited STAT isoform selectivity was also demonstrated using reported FP assays which measure inhibition of native phosphopeptide binding to Stat1. In this assay we found that both **16i** and **21h** show little selectivity for the Stat3 isoform over Stat1 (**16i**, Stat1 IC_{50} = 5.8 ± 0.6 μM *cf*. Stat3 IC_{50} = 2.8 ± 4.3 μM; **21h** Stat1 IC_{50} = 10.9 ± 0.8 μM *cf*. Stat3 IC_{50} = 12.8 ± 2.8 μM, Figure 6 B). Thus, improving STAT isoform selectivity remains a goal for future compound libraries.

To further probe selectivity of **16i**, we conducted a KinomeScan at 5 μM, analogous to approximate IC_{50} values determined in MM cells, to assess potential off-target effects in 132 different cellular kinases, including 37 that possessed SH2 domains. Most encouragingly, this assay revealed only minor off-target effects against SH2 domain containing kinases at 5 μM,

only 2 of the 37 SH2 domain-containing kinases displayed greater than 25 % inhibition of kinase activity. Of note, known upstream regulators of STAT activity, such as JAK1, JAK2, JAK3, TYK2 and SRC, were not inhibited by **16i** (relative activity between 84 and 100 %). A full list of kinases screened and summary of relative inhibition can be found in the supplementary materials.

Given the activity profile of **16i,** we assessed this compound in primary MM patient samples. Encouragingly, **16i** demonstrated activity against malignant plasma cells (CD138+) from primary MM patient samples (Figure 7A), with 20 μM treatment reducing MM tumour cell viability by over 50% in 3 patient samples. Furthermore, at doses exceeding 20 μM, **16i** demonstrated little activity against non-MM (CD138-) cells (Figure 7B). Furthermore, at doses of 30 μM, **16i** had little effect on haematopoietic progenitor colony formation, suggesting that this compound does not inhibit the ability of normal haematopoietic progenitors to proliferate or form distinct colonies (Figure 7C). Taken together, our analysis of **16i** in the context of primary MM patient samples revealed a therapeutic window. Furthermore, although data presented here suggests that **21h** may be a less selective inhibitor as compared to **16i**, it remains an intriguing anti-cancer compound, displaying potent *in vitro* cytotoxic effects in MM cell lines at low μM concentrations.

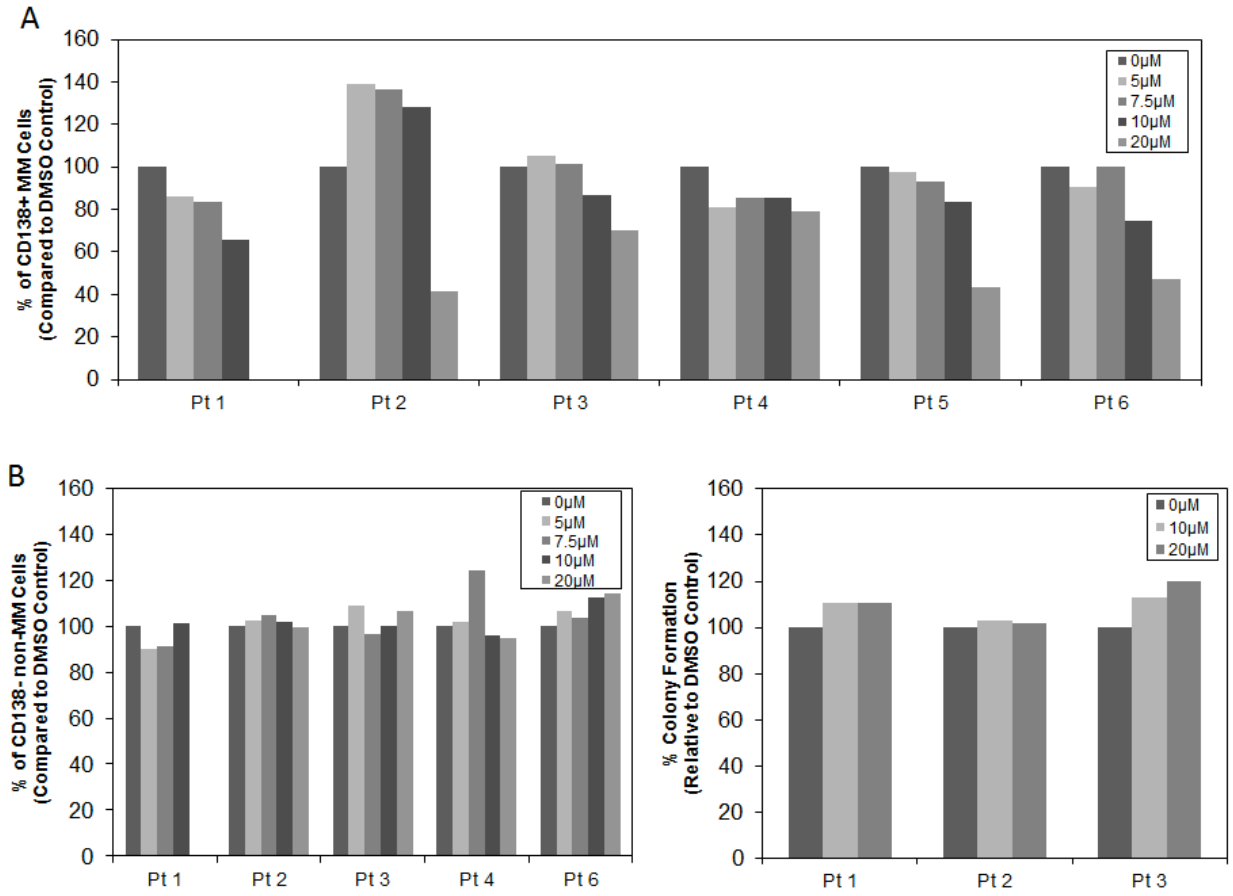

Figure 7. Activity of **16i** against primary MM patient samples. Mononuclear cells (MNC) from MM patients were obtained by Ficoll-Paque separation of 6 patient derived bone marrow aspirates. Samples were cultured and treated with **16i** followed by staining with antibodies against CD138 (MM cell surface marker) or Annexin V (apoptosis). Results are presented as the decrease in CD138+ cell population, representing MM cells (**A**), and decrease in CD138- cell population, representing non-MM cells (**B** left). Alternatively, isolated MNCs were cultured in MethoCult (StemCell Technologies), and treated with **16i** to evaluate the activity of this agent on healthy hematopoietic progenitor colony formation (**B** right).

DISCUSSION AND CONCLUSIONS

We have presented a novel library of salicylic acid-based small molecule Stat3 inhibitors that offer promising Stat3-SH2 binding affinity and anti-MM activity. Lead compounds, **16i** and **21h**, offer improved *in vitro* binding activity over precursors, **7** and **9**, respectively, and improved anti-cancer whole cell activity. *In silico* binding evidence suggested that these compounds bound with greater efficiency to the Stat3 SH2 domain. While NMR and X-ray crystallographic structural studies are ongoing to identify exact binding modes, we can deduce from the presented SAR is that Stat3's SH2 domain might be accommodating of larger, tetrapodal analogs of the **7** and **9** scaffolds. The caveat however, is that this modification appears to reduce STAT isoform selectivity. Both **16i** and **21h** were shown to disrupt phopohopeptide:Stat3 protein complexes, inhibit Stat3 phosphorylation as well as block target gene transcription. Moreover, both compounds have significant anti-MM activity, potently decreasing MM cell viability and promoting the induction of apoptosis. While compound **21h** was the more potent inhibitor, further studies to identify potential off-target effects must be undertaken. Although not as potent, **16i** was shown to have a more favorable toxicity profile, with no observed cytotoxicity in healthy hematopoietic cells or in MM cell lines that harbor minimal pStat3. Furthermore, we have demonstrated that lead agent **16i** has minimal effects against a panel of cellular kinases *in vitro*, suggesting that this Stat3 inhibitor is not likely interacting with kinases to inhibit Stat3 activation. Thus, while we cannot claim that the anti-MM activity of lead agents is a sole result of Stat3 inhibition, evidence does suggest that anti-Stat3 activity does a play a role in the observed biological results. Ongoing biological studies aim to delineate the exact target or combination of targets to better explain the promising results presented herein. Further

experiments are underway to characterize the therapeutic utility of both **16i** and **21h** in *in vivo* studies to identify a Stat3 inhibitor candidate suitable for advanced preclinical trials in MM.

ACKNOWLEDGEMENTS

This work was supported by the National Science Engineering Research Councils (NSERC) (PTG), University of Toronto (PTG), and by an NSERC CGSD fellowship (BDGP).

Corresponding authors

Patrick T. Gunning, E-mail: patrick.gunning@utoronto.ca; Tel.: 905-828-5354; Fax: 905-569-5425.

Suzanne Trudel, E-mail: strudel@uhnres.utoronto.ca; Tel.: 416-946-4501 (Ext 4566).

Supporting Information Available: Chemical methods, characterization, and additional information for biological assays.

Abbreviations

SH2	Src Homology 2 domain
STAT3	Signal Transducer and Activator of Transcription (3) Protein
cPARP	cleaved Poly ADP-ribose polymerase
GM-CSF	Granulocyte macrophage colony-stimulating factor
MM	Multiple Myeloma
MTT	3-(4,5-Dimethylthiazol-2-yl)-2,5-diphenyltetrazolium bromide, a yellow tetrazole

MTS	(3-(4,5-dimethylthiazol-2-yl)-5-(3-carboxymethoxyphenyl)-2-(4-sulfophenyl)-2H-tetrazolium)
siRNA	small interfering RNA
RNAi	RNA interference
PI	Propidium iodide
FP	Fluorescence Polarization
MNC	Mononuclear cells
GOLD	Genetically Optimized Ligand Docking

REFERENCES

1. Haftchenary, S.; Avadisian, M.; Gunning, P. T. Inhibiting aberrant Stat3 function with molecular therapeutics: A progress report. *Anticancer Drugs* **2011**, *22,* 115-127.

2. Page, B. D. G.; Ball, D. P.; Gunning, P. T. Signal transducer and activator of transcription 3 inhibitors: a patent review. *Exp. Opin. Ther. Pat.* **2011**, *21,* 65-83.

3. Fletcher, S.; Turkson, J.; Gunning, P. T. Molecular approaches towards the inhibition of the Signal Transducer and Activator of Transcription 3 (Stat3) Protein. *ChemMedChem*, **2008**, *3*, 1159-1168.

4. Fletcher, S.; Drewry, J. A.; Shahani, V. M.; Page, B. D. G.; Gunning, P. T. Molecular disruption of oncogenic signal transducer and activator of transcription 3 (STAT3) protein. *Biochem. Cell Biol.* **2009**, *87,* 825-833.

5. Bromberg, J. F.; Wrzeszczynska, M. H.; Devgan, G.; Zhao, Y.; Pestell, R. G.; Albanese, C.; Darnell Jr., J. E. Stat3 as an oncogene. *Cell* **1999**, *98,* 295-303.

6. Bowman, T.; Garcia, R.; Turkson, J.; Jove, R. STATs in oncogenesis. *Oncogene* **2000**, *19,* 2474-2488.

7. Bromberg, J.; Darnell Jr., J. E. The role of STATs in transcriptional control and their impact on cellular function. *Oncogene* **2000**, *19,* 2468-2473.

8. Raab, M. S.; Podar, K.; Breitkreutz, I.; Richardson, P. G.; Anderson, K. C. Multiple myeloma. *The Lancet* **2009**, *374,* 324-339.

9. Munshi, N. C. Plasma cell disorders: an historical perspective. *Hematology / the Education Program of the American Society of Hematology.American Society of Hematology.Education Program* **2008**, 297.

10. Singhal, S.; Mehta, J.; Desikan, R.; Ayers, D.; Roberson, P.; Eddlemon, P.; Munshi, N.; Anaissie, E.; Wilson, C.; Dhodapkar, M.; Zeldis, J.; Barlogie, B.; Siegel, D.; Crowley, J. Antitumor activity of thalidomide in refractory multiple myeloma. *N. Engl. J. Med.* **1999**, *341,* 1565-1571.

11. Badros, A.; Gahres, N. Bortezomib, thalidomide, and dexamethasone for relapsed multiple myeloma: Add it up and wait. *Clinical Advances in Hematology and Oncology* **2005**, *3,* 916-917.

12. Alas, S.; Bonavida, B. Inhibition of constitutive STAT3 activity sensitizes resistant non-Hodgkin's lymphoma and multiple myeloma to chemotherapeutic drug-mediated apoptosis. *Clinical Cancer Research* **2003**, *9,* 316-326.

13. Catlett-Falcone, R.; Landowski, T. H.; Oshiro, M. M.; Turkson, J.; Levitzki, A.; Savino, R.; Ciliberto, G.; Moscinski, L.; Fernández-Luna, J. L.; Nuñez, G.; Dalton, W. S.; Jove, R. Constitutive activation of Stat3 signaling confers resistance to apoptosis in human U266 myeloma cells. *Immunity* **1999**, *10,* 105-115.

14. Lin, L.; Benson Jr., D. M.; Deangelis, S.; Bakan, C. E.; Li, P. -.; Li, C.; Lin, J. A small molecule, LLL12 inhibits constitutive STAT3 and IL-6-induced STAT3 signaling and exhibits potent growth suppressive activity in human multiple myeloma cells. *Intl. J. Cancer* **2012**, *130,* 1459-1469.

15. Fletcher, S.; Page, B. D. G.; Zhang, X.; Yue, P.; Li, Z. H.; Sharmeen, S.; Singh, J.; Zhao, W.; Schimmer, A. D.; Trudel, S.; Turkson, J.; Gunning, P. T. Antagonism of the Stat3-Stat3 Protein Dimer with Salicylic Acid-Based Small Molecules. *ChemMedChem* **2011**, *6*, 1459-1470.

16. Heim, M. H.; Kerr, I. M.; Stark, G. R.; Darnell Jr., J. E. Contribution of STAT SH2 groups to specific interferon signaling by the Jak-STAT pathway. *Science* **1995**, *267,* 1347-1349.

17. Gunning, P. T.; Glenn, M. P.; Siddiquee, K. A.; Katt, W. P.; Masson, E.; Sebti, S. M.; Turkson, J.; Hamilton, A. D. Targeting protein-protein interactions: suppression of Stat3 dimerization with rationally designed small-molecule, nonpeptidic SH2 domain binders. *ChemBioChem* **2008**, *9,* 2800-2803.

18. Becker, S.; Groner, B.; Müller, C. W. Three-dimensional structure of the Stat3β homodimer bound to DNA. *Nature* **1998**, *394,* 145-151.

19. Siddiquee, K. A. Z.; Gunning, P. T.; Glen, M.; Katt, W. P.; Zhang, S.; Schroeck, C.; Sebti, S. M.; Jove, R.; Hamilton, A. D.; Turkson, J. An oxazole-based small-molecule stat3 inhibitor modulates stat3 stability and processing and induces antitumor cell effects. *ACS Chem. Biol.* **2007**, *2,* 787-798.

20. Mandai, P. K.; Lião, W. S. -.; McMurray, J. S. Synthesis of phosphatase-stable, cell-permeable peptidomimetic prodrugs that target the SH2 domain of Stat3. *Org. Lett.* **2009**, *11,* 3394-3397.

21. Coleman IV, D. R.; Ren, Z.; Mandal, P. K.; Cameron, A. G.; Dyer, G. A.; Muranjan, S.; Campbell, M.; Chen, X.; McMurray, J. S. Investigation of the binding determinants of phosphopeptides targeted to the Src homology 2 domain of the signal transducer and activator of transcription 3. Development of a high-affinity peptide inhibitor. *J. Med. Chem.* **2005**, *48,* 6661-6670.

22. Shahani, V. M.; Yue, P.; Fletcher, S.; Sharmeen, S.; Sukhai, M. A.; Luu, D. P.; Zhang, X.; Sun, H.; Zhao, W.; Schimmer, A. D.; Turkson, J.; Gunning, P. T. Design, synthesis, and *in vitro* characterization of novel hybrid peptidomimetic inhibitors of STAT3 protein. *Bioorg. Med. Chem.* **2011**, *19*, 1823-1838.

23. Gunning, P. T.; Katt, W. P.; Glenn, M.; Siddique, K.; Kim, J. S.; Jove, R.; Sebti, S. M.; Turkson, J.; Hamilton, A. D. Isoform selective inhibition of STAT1 or STAT3 homo-dimerization via peptidomimetic probes: Structural recognition of STAT SH2 domains. *Bioorg. Med. Chem. Lett.* **2007**, *17,* 1875-1878.

24. Hao, W.; Hu, Y.; Niu, C.; Huang, X.; Chang, C. -. B.; Gibbons, J.; Xu, J. Discovery of the catechol structural moiety as a Stat3 SH2 domain inhibitor by virtual screening. *Bioorg. Med. Chem. Lett.* **2008**, *18,* 4988-4992.

25. Shahani, V. M.; Yue, P.; Haftchenary, S.; Zhao, W.; Lukkarila, J. L.; Zhang, X.; Ball, D.; Nona, C.; Gunning, P. T.; Turkson, J. Identification of purine-scaffold small-molecule inhibitors of stat3 activation by QSAR studies. *ACS Med. Chem. Lett.* **2011**, *2,* 79-84.

26. Fletcher, S.; Singh, J.; Zhang, X.; Yue, P.; Page, B. D. G.; Sharmeen, S.; Shahani, V. M.; Zhao, W.; Schimmer, A. D.; Turkson, J.; Gunning, P. T. Disruption of transcriptionally active stat3 dimers with non-phosphorylated, salicylic acid-based small molecules: Potent in vitro and tumor cell activities. *ChemBioChem* **2009**, *10,* 1959-1964.

27. Page, B. D. G.; Fletcher, S.; Yue, P.; Li, Z.; Zhang, X.; Sharmeen, S.; Datti, A.; Wrana, J. L.; Trudel, S.; Schimmer, A. D.; Turkson, J.; Gunning, P. T. Identification of a non-phosphorylated, cell permeable, small molecule ligand for the Stat3 SH2 domain. *Bioorg. Med. Chem. Lett.* **2011**, *21,* 5605-5609.

28. Zhang, X.; Yue, P.; Fletcher, S.; Zhao, W.; Gunning, P. T.; Turkson, J. A novel small-molecule disrupts Stat3 SH2 domain-phosphotyrosine interactions and Stat3-dependent tumor processes. *Biochem. Pharmacol.* **2010**, *79,* 1398-1409.

29. Siddiquee, K.; Zhang, S.; Guida, W. C.; Blaskovich, M. A.; Greedy, B.; Lawrence, H. R.; Yip, M. L. R.; Jove, R.; McLaughlin, M. M.; Lawrence, N. J.; Sebti, S. M.; Turkson, J. Selective chemical probe inhibitor of Stat3, identified through structure-based virtual screening, induces antitumor activity. *Proc. Natl. Acad. Sci. U. S. A.* **2007**, *104,* 7391-7396.

30. Zhang, X.; Yue, P.; Fletcher, S.; Zhao, W.; Gunning, P. T.; Turkson, J. A novel small-molecule disrupts Stat3 SH2 domain-phosphotyrosine interactions and Stat3-dependent tumor processes. *Biochem. Pharmacol.* **2010**, *79,* 1398-1409.

31. Zhang, X.; Yue, P.; Page, B. D. G.; Li, T.; Zhao, W.; Namanja, A. T.; Paladino, D.; Zhao, J.; Chen, Y.; Gunning, P. T.; Turkson, J. Orally bioavailable small-molecule inhibitor of transcription factor Stat3 regresses human breast and lung cancer xenografts. *Proc. Natl. Acad. Sci. U. S. A.* **2012**, *109,* 9623-9628.

32. Totrov, M.; Abagyan, R. Flexible protein-ligand docking by global energy optimization in internal coordinates. *Proteins: Structure, Function and Genetics* **1997**, *29,* 215-220.

33. Jones, G.; Willett, P.; Glen, R. C.; Leach, A. R.; Taylor, R. Development and validation of a genetic algorithm for flexible docking. *J. Mol. Biol.* **1997**, *267,* 727-748.

34. Schust, J.; Berg, T. A high-throughput fluorescence polarization assay for signal transducer and activator of transcription 3. *Anal. Biochem.* **2004**, *330,* 114-118.

35. Greil, R.; Fasching, B.; Loidl, P.; Huber, H. Expression of the c-myc proto-oncogene in multiple myeloma and chronic lymphocytic leukemia: An in situ analysis. *Blood* **1991**, *78,* 180-191.

Table of Contents Graphic